

Constitutive Expression of Murine Decay-Accelerating Factor 1 Is Controlled by the Transcription Factor Sp1¹

David M. Cauvi, Gabrielle Cauvi, and K. Michael Pollard²

The complement regulatory protein decay-accelerating factor (DAF or CD55) protects host tissue from complement-mediated injury by inhibiting the classical and alternative complement pathways. Besides its role in complement regulation, DAF has also been shown to be a key player in T cell immunity. Modulation of DAF expression could therefore represent a critical regulatory mechanism in both innate and adaptive immune responses. To identify and characterize key transcriptional regulatory elements controlling mouse *Daf1* expression, a 2.5-kb fragment corresponding to the 5' flanking region of the mouse *Daf1* gene was cloned. Sequence analysis showed that the mouse *Daf1* promoter lacks conventional TATA and CCAAT boxes and displays a high guanine and cytosine content. RACE was used to identify one major and two minor transcription start sites 47, 20, and 17 bp upstream of the translational codon. Positive and negative regulatory regions were identified by transiently transfecting sequential 5' deletion constructs of the 5' flanking region into NIH/3T3, M12.4, and RAW264.7 cells. Mutational analyses of the promoter region combined with Sp1-specific ELISA showed that the transcription factor Sp1 is required for basal transcription and LPS-induced expression of the *Daf1* gene. These findings provide new information on the regulation of the mouse *Daf1* promoter and will facilitate further studies on the expression of *Daf1* during immune responses. *The Journal of Immunology*, 2006, 177: 3837–3847.

Decay-accelerating factor (DAF,³ CD55) is a member of the complement-regulatory protein family that protects cells from attack by autologous complement proteins (1). DAF functions to accelerate the dissociation of the preformed C3/C5 convertase complexes of both the classical and alternative pathways of complement, thus blocking complement activation (2). Two recent studies have shown that DAF also acts as a negative modulator of T cell immunity (3, 4) by limiting T cell hyperresponsiveness induced by alternative pathway C3 activation during T cell-APC interactions (4). Besides its major involvement in both the innate and adaptive immune systems, DAF also has noncomplement-related functions because it has been shown to be a receptor for several viral and bacterial pathogens (5), and more recently to be the cellular ligand for the leukocyte Ag CD97, a member of the epidermal growth factor family (6). The DAF-CD97 interaction appears to be involved in inflammatory responses (7, 8). DAF also has the capacity to act as a signal-transducing molecule in T cells (9) and monocytes (10) via interaction with src protein tyrosine kinases (11).

In humans, DAF is a GPI-anchored membrane glycoprotein encoded by a single gene which maps to q32 on chromosome 1 (12). It is widely expressed on the surface of all major circulating blood cells and numerous epithelial and endothelial cells (13, 14). The

genomic structure of mouse DAF consists of two genes laying head-to-tail along chromosome 1 (15), with the *Daf1* (Daf-GPI) gene located 5' to the *Daf2* (Daf-transmembrane) gene. Studies with *Daf1* knockout mice have revealed that *Daf1* is broadly expressed in most tissues, while *Daf2* expression is restricted to the testis and CD11c-positive splenic dendritic cells (16, 17).

Expression of DAF is influenced in a number of ways. Constitutive expression can vary depending on tissue (16) and cell type (18). In the mouse, estrogen induces *Daf1* expression in uterine tissue showing that the two mouse *Daf* genes can be independently regulated in a single tissue (19). In human cells, DAF expression is modulated by cytokines such as IL-1, IL-6, TNF- α , TGF- β 1, and IFN- γ (20–22), prostaglandins like PGE₂ (23), and tissue-specific factors (24). Although there is evidence that DAF mRNA stability can be affected by tissue-specific factors (24) and inflammation (25), a number of studies have suggested that the primary modulation of expression appears to be at the level of transcription (22–24, 26, 27).

The growing importance of DAF, not only as a key player in the innate immune system, but also as a critical component of T cell immunity, suggests that regulation of its expression may have significant effects on health and disease. The human DAF promoter has been identified, the transcription start site mapped, and regions of potential transcriptional regulation discussed (18, 28). In contrast, nothing is known regarding the promoter structure or mechanisms underlying the transcriptional regulation of murine *Daf* gene expression.

The aim of this report was to investigate the transcriptional regulation of the murine *Daf1* promoter. To this end, a 2.5-kb genomic fragment of the *Daf1* 5' flanking region was isolated, analyzed, and cloned into a luciferase-containing reporter vector. Transfection into murine embryo fibroblasts (NIH/3T3), mature B cells (M12.4), and macrophages (RAW264.7) demonstrated that this fragment contains a functional promoter capable of driving luciferase activity. Regions that positively and negatively regulate the *Daf1* basal promoter activity were then identified using 5' serial deletions of the 2.5-kb 5' flanking region. The effect of sequence-specific mutations on transcription, as well as transcription

Department of Molecular and Experimental Medicine, W. M. Keck Autoimmune Disease Center, The Scripps Research Institute, La Jolla, CA 92037

Received for publication April 21, 2006. Accepted for publication June 21, 2006.

The costs of publication of this article were defrayed in part by the payment of page charges. This article must therefore be hereby marked *advertisement* in accordance with 18 U.S.C. Section 1734 solely to indicate this fact.

¹ This work was supported by National Institutes of Health Grants ES07511, ES09802, and ES08080, and The Stein Endowment Fund. D.M.C. is an Arthritis National Research Foundation Grant Recipient.

² Address correspondence and reprint requests to Dr. K. Michael Pollard, Department of Molecular and Experimental Medicine, MEM131, The Scripps Research Institute, 10550 North Torrey Pines Road, La Jolla, CA 92037. E-mail address: mpollard@scripps.edu

³ Abbreviations used in this paper: DAF, decay-accelerating factor; RT, room temperature; GC, guanine and cytosine; TF, transcription factor.

factor binding to selected oligonucleotide sequences, were used to demonstrate that the transcription factor Sp1 plays a critical role in regulating the basal transcription of murine Daf1. Finally, Sp1 was shown to be important for LPS-enhanced expression of Daf1.

Materials and Methods

Cloning and sequence analysis

Genomic DNA was extracted from DBA/2 mice. PCRs were performed using KOD Hot start DNA polymerase (Novagen) under the following conditions: 94°C (30 s), 62°C (30 s), and 68°C (3 min). Primers were designed according to the mouse genome database (29): forward, 5'-GCATCTCGAGACACAAAACCTCGCCAGCAC-3' (*Xho*I site underlined) and reverse, 5'-GCATAAGCTTACAGCAGCAACAGAGACAG-3' (*Hind*III site underlined). PCR products were separated using a 1.0% agarose gel, extracted, and then cloned into the pGL3-basic vector (Promega). Sequencing, using an ABI PRISM 3100 sequencer, was performed in both directions with primers from the vector flanking sequence. DBA/2 genomic DNA sequence was identical to that of the C57BL/6 sequence (Ensembl gene ID no. ENSMUS0000026399). Genomatix's ElDorado software (Genomatix Software) was used to identify the putative Daf1 promoter region and to search transcription factor databases to discover potential regulatory elements. Sequences showing over 85% similarity to reported transcription factor consensus sites were considered. BioEdit Sequence Alignment Editor Software (version 6.0.5) was used to align and compare the murine Daf1 sequence to those of rat, human, and chimpanzee.

Mapping of the transcription start site

Single-cell suspensions were obtained from DBA/2/J spleen by mashing the organ in RPMI 1640 containing 10% FCS. Total RNA isolation was performed using TRIzol Reagent (Invitrogen Life Technologies) according to the manufacturer's protocol. RACE PCR was performed as directed in the GeneRacer kit protocol (Invitrogen Life Technologies). Reverse transcription was then performed using SuperScript III followed by PCR amplification of the cDNA 5' end using Platinum DNA Polymerase High Fidelity (Invitrogen Life Technologies). The following primers were used for amplification: Gene Racer forward primer and Daf1 race reverse 5'-CCGCGTACAGTTGGGGACAGCAGCAAC-3'. The PCR product was separated by agarose gel electrophoresis, extracted, and inserted into the pCR4-TOPO plasmid vector. Twelve colonies were picked and submitted for sequencing using M13 Reverse and T7 Primers.

Cell culture

The NIH/3T3 embryo fibroblast cell line (ATCC CRL-1658) and RAW 264.7 murine macrophage cell line (ATCC TIB-71) were obtained from American Type Culture Collection (ATCC), and maintained at 37°C in a humidified 5% CO₂ atmosphere in high glucose DMEM with 2 mM L-

glutamine (Invitrogen Life Technologies) supplemented with 10% (v/v) FBS (Omega Scientific) and penicillin-streptomycin.

M12.4 mature mouse B cell line was a gift from Prof. R. H. Scheuermann (University of Texas Southwestern Medical Center, Dallas, TX), and was cultured in IMEM with 2 mM L-glutamine (Invitrogen Life Technologies) supplemented with 5% FBS (Omega Scientific), penicillin-streptomycin, and 50 μM 2-ME.

Schneider's *Drosophila melanogaster* cell line (SL2; ATCC CRL-1963) was obtained from the ATCC, and maintained at 24°C in Schneider's *Drosophila* medium (Invitrogen Life Technologies) supplemented with 10% FBS (Omega Scientific).

RNA isolation and reverse transcription

Total RNA extraction from NIH/3T3, M12.4, and RAW 264.7 cell lines was performed using TRIzol reagent (Invitrogen Life Technologies). RNA was denatured at 65°C for 5 min, placed on ice, and reverse transcribed in a total volume of 20 μl using random hexamers, dNTPs, RNase inhibitor (RNaseOUT; Invitrogen Life Technologies), and 200 U of SuperScript III reverse transcriptase (Invitrogen Life Technologies). PCR was conducted under the following conditions: 94°C (30 s), 53°C (30 s), and 72°C (30 s) and products were separated using a 1.5% agarose gel and visualized by ethidium bromide. The following primers were used for amplification: Daf1 forward, 5'-CTTGACAGTTTTGCATGTGA-3' and Daf1 reverse, 5'-TCCATTCTTCTTGACAGTCT-3'; β-actin forward, 5'-TGGGAATCCTGTGGCATCCATGAAACT-3' and β-actin reverse, 5'-TGTAACCGCAGCTCAGTAACAGTCCG-3'. For real-time quantitative PCR, RNA was extracted with TRIzol reagent (Invitrogen Life Technologies) from NIH/3T3, M12.4, and RAW 264.7 cells exposed to 10 μg/ml LPS (Sigma-Aldrich) or medium alone for 24 h. Reverse transcription was then performed from 1 μg of RNA as described above and the resulting cDNA was diluted 10-fold in 10 mM Tris (pH 8.0) containing 1 mM EDTA (Tris-EDTA buffer; Ambion), and stored at -80°C.

Promoter constructs

Various deletion constructs of the murine Daf1 promoter were generated from DBA/2 genomic DNA by PCR amplification using oligonucleotide primers (summarized in Table I) containing *Xho*I (forward) and *Hind*III (reverse) restriction enzyme sites for cloning purposes. PCR products were separated on agarose gels, digested with *Xho*I/*Hind*III enzymes, and then cloned into the pGL3-basic vector (Promega). Substitution mutations were performed by using two rounds of PCR amplification. For example: Sp1-A mutant was produced by using the PCR product from oligonucleotides p(-619/+85)/RSp1-A mut plus the PCR product from oligonucleotides FSp1-A mut/pRev as template in a second-stage PCR using primers p(-619/+85) and pRev. All mutants were prepared by using a similar strategy. All plasmids were purified using an endotoxin-free plasmid kit (Qiagen). The sequence of all constructs was confirmed using an ABI PRISM 3100 sequencer.

Table I. Sequence of PCR oligonucleotides used in this study to generate deletion and mutant constructs^a

| Name | Orientation | Construct | Oligonucleotide Sequence |
|---------------|-------------|-----------|--|
| p(-2408/+85) | Forward | Deletion | 5'-GCATCTCGAGACACAAAACCTCGCCAGCAC-3' |
| p(-1746/+85) | Forward | Deletion | 5'-GCATCTCGAGAGTGAATGAGGTCACAGAGA-3' |
| p(-1104/+85) | Forward | Deletion | 5'-GCATCTCGAGCAGACCCAGACACACAAAG-3' |
| p(-619/+85) | Forward | Deletion | 5'-GCATCTCGAGGCTAAGAAGGTGACTCCTCA-3' |
| p(-337/+85) | Forward | Deletion | 5'-GCATCTCGAGCACTCAGCACACCAGAGTT-3' |
| p(-179/+85) | Forward | Deletion | 5'-GCATCTCGAGCCCTGGGTGAAGTAGA-3' |
| p(-18/+85) | Forward | Deletion | 5'-GCATCTCGAGTCTCTTCTACCTGGGCTAT-3' |
| pRev | Reverse | Deletion | 5'-GCATAAGCTTACAGCAGCAACAGAGACAG-3' |
| FSp1-A mut | Forward | Mutation | 5'-GCTAGAGGCCAGGCACatGcatTCATTAAATGAGGGAAC-3' |
| RSp1-A mut | Reverse | Mutation | 5'-GTTCCCTCATTAATGAatGcatGTGCTGGCCTTAGC-3' |
| FSp1-B mut | Forward | Mutation | 5'-CTTGACAGCAGGCTGcatCACATAGGGTGACGAGGGCC-3' |
| RSp1-B mut | Reverse | Mutation | 5'-GGCCCTCGTCAACCtAtGTGatGCAGCCTGCGTGCAAG-3' |
| FSp1-C mut | Forward | Mutation | 5'-GTGACGAGGGCCCTGcatCGcatCGCCACAGCTGCTCAAT-3' |
| RSp1-C mut | Reverse | Mutation | 5'-ATTGAGCAGCTGTGGCgatGCGatGCAGGGCCCTCGTCAC-3' |
| FCREB mut | Forward | Mutation | 5'-CTGCCACCCAGGGatACatGGGCCCTGC-3' |
| RCREB mut | Reverse | Mutation | 5'-GCAGGGCCcatGTatCCCTGGGTGGGCAG-3' |
| FCREB/Sp1 mut | Forward | Mutation | 5'-CTGatCACatAGGGatGGGCCCTGC-3' |
| RCREB/Sp1 mut | Reverse | Mutation | 5'-GCAGGGCCcatGTatCCCTatGTGatCAG-3' |

^a Oligonucleotide sequences corresponding to the template cDNA are represented in uppercase. Mutations are depicted in bold lowercase. *Xho*I and *Hind*III restriction enzyme sites are single or double underlined, respectively.

Reprint requests: Richard F. Spaide, 460 Park Avenue, 5th Floor, New York, NY 10022; e-mail: vrnmny@aol.com

Transient transfection and luciferase assay
Cells were plated the day before transfection in 12-well plates at 2.1×10^5 cells/well for NIH/3T3 cells and in 24-well plates at 2.5×10^5 cells/well for M12.4 and RAW 264.7 cells. Cells were washed twice with PBS and transfected with various firefly luciferase reporter vectors using Lipofectamine 2000 (Invitrogen Life Technologies) according to the manufacturer's instructions with a 10:1 Lipofectamine 2000-to-DNA ratio. pRL-TK vector (Promega) encoding *Renilla* luciferase was added in each transfection as an internal control plasmid. After 48 h of incubation, cells were harvested, lysed with Passive Lysis Buffer (Promega), and promoter activities were determined using the Dual-Luciferase Assay System (Promega). When required, cells were stimulated 24 h posttransfection with 10 μ g/ml LPS. After an additional 24 h, cells were harvested and promoter activities were analyzed as described above. Luciferase activities were measured with the Clarity Luminescence Microplate Reader (Bio-Tek Instruments) and firefly luciferase activities were normalized to *Renilla* luciferase activities.

SL2 cells were plated the day before transfection at 2.5×10^5 cells/well in 24-well plates and transfected as described above with various firefly luciferase reporter vectors along with differing amounts of either the empty vector pPac or the Sp1-containing vector pPacSp1. Firefly and *Renilla* luciferase activities were measured as described above. Both pPac and pPacSp1 were provided by Prof. G. Suske (Philipps University, Marburg, Germany).

Real-time quantitative PCR

Daf1 and cyclophilin A primers and probes were designed with Beacon designer 3.01 software (Premier Biosoft International). The primers used were as follows: Daf1 forward primer, 5'-CTTGACAGTTTGCATGTGA-3'; Daf1 reverse primer, 5'-TCCATTCTTCTTGGACAGTCT-3'; cyclophilin A forward primer, 5'-GGCCGATGACGAGCCC-3'; cyclophilin A reverse primer, 5'-TGTCTTTGGAACCTTTGTCTGC-3'. The following dual-labeled probes were obtained from Integrated DNA Technologies: Daf1, 5'-FAM-CTACTTGACATAGCCAACGAGAGTTACGAAGA BHQ1-3'; cyclophilin A, 5'-FAM-TGGGCCGCGTCTCCTTCGABHQ1-3'. Cyclophilin A standards were cloned into pGEMTeasy (Promega) and a standard curve was generated for each experiment. All samples and standards were analyzed in triplicate. PCR amplification were performed in a total volume of 25 μ l containing 1.0 mM Tris-HCl, 5 mM KCl, 200 μ M dNTPs, 100 ng of forward and reverse primers, 4 mM MgCl₂, 0.625 U of AmpliTaq Gold (Applied Biosystems), and 2.5 pM Daf1 or cyclophilin A dual-labeled probes. The reactions conditions were 95°C for 10 min followed by 45 cycles of 30 s at 94°C, 30 s at 60°C, and 30 s at 72°C and conducted using the iCycler iQ (Bio-Rad).

Transcription factor ELISA

Transcription factor ELISA were conducted according to Hibma et al. (30) with some modifications. Both parent and complementary single-strand oligonucleotides encompassing the wild-type or mutated Sp1-binding site consensus sequences were obtained from Integrated DNA Technologies. Each oligonucleotide was purified using PAGE purification and the 5' end of the parent oligonucleotide was either biotinylated or not by Integrated DNA Technologies (Table II). Double-strand oligonucleotides were obtained by annealing either the biotinylated or the nonbiotinylated parent strand with the complementary strand by heating at 100°C for 10 min in Tris-EDTA buffer (10 mM Tris-HCl, 1 mM EDTA (pH 7.8)) and gradual cooling to 25°C. Nuclear extracts were prepared from NIH/3T3, M12.4, and RAW264.7 cells using the NE-PER Extraction Reagents (Pierce) supplemented with the Halt Protease Inhibitor mixture (Pierce) according to

the manufacturer's instructions. Protein concentration of the nuclear extract was determined using Bio-Rad protein assay. rSp1 was purchased from Promega. Immulon 2B immunoassay plates (Thermo) were coated overnight at 37°C with 100 μ l of a 10 μ g/ml solution of ImmunoPure Streptavidin (Pierce) resuspended in distilled water. Plates were washed three times at room temperature (RT) for 5 min with PBST. Each well was blocked for 1 h with 3% BSA diluted in 12.5 mM Tris-HCl (pH 7.6), 1.25 mM MgCl₂, 50 mM NaCl, 0.5 mM EDTA, 0.5 mM DTT (freshly added), and 4% glycerol (binding buffer). Subsequently, 100 μ l of a 1 μ g/ml solution of double-strand biotinylated wild-type or mutant oligonucleotides were added per well and allowed to attach for 30 min at 37°C on a shaking platform. Either nuclear extract or rSp1 diluted in the binding buffer supplemented with 0.05 mM double-strand poly(dI-dC) (Amersham Biosciences) were added and incubated for 1 h at RT. In competition assays, rSp1 was preincubated with increasing amounts of nonbiotinylated oligonucleotide for 45 min at RT and this mixture was then added to the well coated with the biotinylated wild-type oligonucleotide for 1 h at RT. Plates were washed three times at RT for 5 min with PBST. For detection, 100 ng/well of either anti-Sp1 (rabbit polyclonal; Upstate Biotechnology) Ab or an irrelevant Ab (rabbit polyclonal) diluted in binding buffer was added and incubated for 1 h at RT. After washing, an HRP-conjugated anti-rabbit Ab diluted in binding buffer was added and incubated for 45 min at RT. Wells were washed three times at RT for 5 min with PBST and, finally, 100 μ l of ABTS substrate was added per well and color development was measured at 405 nm using a Vmax microplate reader (Molecular Devices).

Results

Cloning and analysis of the 5'-flanking region of the mouse

Daf1 gene

A genomic fragment of ~2.4 kb from the ATG codon corresponding to the 5'-flanking region of the *Daf1* gene was cloned. Genomatix's EIDorado software was used to identify a 600-nt promoter region consisting of -515 residues upstream and +85 residues downstream of the initiating ATG codon, as well as potentially important regulatory elements representing consensus-binding sites of known transcription factors (Fig. 1). Sequence analysis also revealed that the putative Daf1 promoter lacked conventional TATA and CCAAT boxes. The guanine and cytosine (GC) content of the -2408 to +85 bp sequence was 46% but increased to 58% for the -644 to +85 bp sequence and reached 65% for the -300 to +85 bp sequence. Four potential Sp1-binding sites, at positions -153 to -147, -109 to -103, -84 to -76, and +10 to +16 bp, were found embedded within this latter GC-rich region (Fig. 1).

Identification of mouse *Daf1* transcription start site

TATA-less GC-rich promoters often contain multiple transcriptional start sites (31). To characterize the *Daf1* transcription start site(s), we performed RACE on total cellular RNA from mouse splenocytes. The resulting PCR product (Fig. 2A) was cloned into a pCR4-TOPO vector and sequenced. Ten of 12 clones ended in the sequence AAAACAG (47 bp upstream of the ATG start codon) and consequently the terminal nucleotide A was designated as the major transcriptional start site (Fig. 2B). The two other clones terminated with the sequence GGTCTCT and CTCTTCT

Table II. Sequence of oligonucleotides used in transcription factor ELISA^a

| | | | |
|----------|---------------|-----------------|--|
| wtSp1-B | Parent | Nonbiotinylated | 5'-CGCAGGCTGCCCCACCCAGGGTGACGAG-3' |
| wtSp1-B | Parent | Biotinylated | 5'-Bio-CGCAGGCTGCCCCACCCAGGGTGACGAG-3' |
| wtSp1-B | Complementary | Nonbiotinylated | 5'-CTCGTCACCCTGGGTGGGGCAGCCTGCG-3' |
| mutSp1-B | Parent | Biotinylated | 5'-Bio-CGCAGGCTGC cat CAC cat AGGGTGACGAG-3' |
| mutSp1-B | Complementary | Nonbiotinylated | 5'-CTCGTCACCCT at GTG at GACGCTGCG-3' |
| wtSp1-C | Parent | Nonbiotinylated | 5'-GAGGGCCCTGCCCCGCCGCCACAGC-3' |
| wtSp1-C | Parent | Biotinylated | 5'-Bio-GAGGGCCCTGCCCCGCCGCCACAGC-3' |
| wtSp1-C | Complementary | Nonbiotinylated | 5'-GCTGTGGCGGGGCGGGCAGGGCCCTC-3' |
| mutSp1-C | Parent | Biotinylated | 5'-Bio-GAGGGCCCTGC cat CG cat CGCCACAGC-3' |
| mutSp1-C | Complementary | Nonbiotinylated | 5'-GCTGTGGCC at GCC at GACGGCCCTC-3' |

^aOligonucleotide sequences corresponding to the template cDNA are represented in uppercase. Mutations are depicted in bold lowercase.

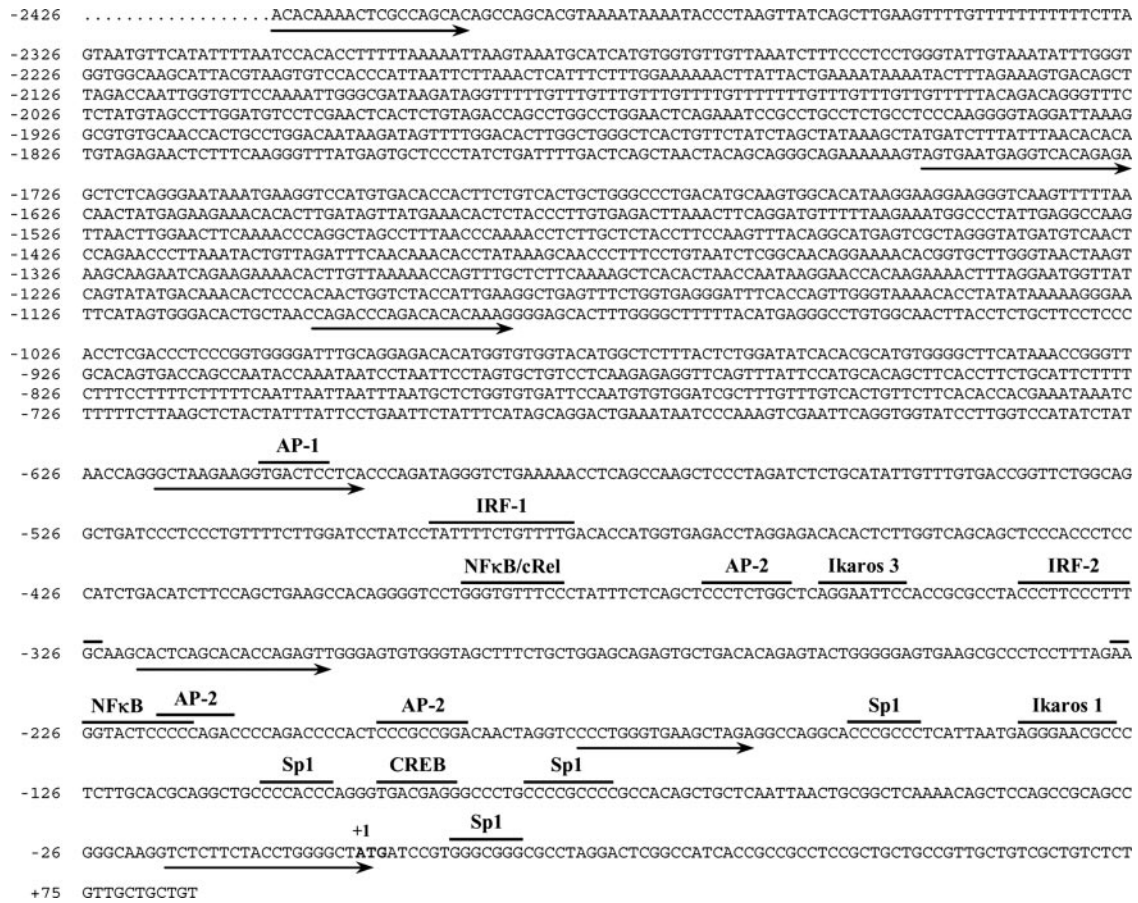


FIGURE 1. Nucleotide sequence of the 5'-flanking region of the *Daf1* gene. Sequences that match consensus-binding sites of known transcription factors are indicated. Numbers designate the nucleotide position relative to the translational start site. The nucleotide A of the ATG codon is denoted +1. Oligonucleotide sequences used to generate 5' deletion constructs shown in Fig. 4 are underlined by an arrow.

(-20 and -17 bp from the ATG codon, respectively). These findings differ from a previous study (15) which identified the *Daf1* transcription start 15 bp upstream of the translational ATG codon.

Identification of transcriptional regulatory regions of mouse *Daf1* gene

Although DAF is expressed in virtually all cells, the level of expression can vary and this property has been used in transcriptional activity studies of the human DAF promoter (18). To help identify possible differences in transcriptional activity of *Daf1* expression, we used three murine cell lines with different levels of expression (Fig. 3A). The highest level of *Daf1* transcript was observed in NIH/3T3 cells, followed by M12.4 cells, with RAW264.7 cells having the lowest expression.

To determine whether the 2.5-kb fragment of the 5' flanking region of mouse *Daf1* (Fig. 1) contained the *Daf1* promoter, we cloned the fragment, designated p(-2408/+85)Luc, into the promoterless pGL3 reporter vector encoding the firefly luciferase. Either this construct or the control pGL3 vector were transfected in NIH/3T3, M12.4, and RAW264.7 cells along with a vector encoding the *Renilla* luciferase as a transfection internal control. In all three cell lines, the 2493-bp DNA fragment was fully capable of inducing luciferase activity (Fig. 3B), indicating that the *Daf1* basal promoter activity is contained within this fragment. To further define the region influencing *Daf1* gene expression, a series of 5'-deletion constructs of the p(-2408/+85)Luc was generated (Fig. 4A), and expressed as percent activity relative to the

p(-2408/+85)Luc luciferase activity (Fig. 4B). Deletion of 660 bp (p(-1746/+85)Luc) or 1302 bp (p(-1104/+85)Luc) did not produce any significant changes in relative luciferase activities. Further, deletion to position -619 (p(-619/+85)Luc) resulted in an increase of the promoter activity in all three cell lines suggesting the presence of negative regulatory element(s) within the -1104- to -619-bp region. The magnitude of the increase was much larger in RAW264.7 cells (193.5%) than in NIH/3T3 or M12.4 cells (74 and 109.4%, respectively). Additional deletions of 282 bp (p(-337/+85)Luc) and 440 bp (p(-179/+85)Luc) resulted in a gradual decrease of the promoter activity to a level comparable to the full-length construct, p(-2408/+85)Luc, indicating that the region between -619 and -179 bp contains positive regulatory element(s) involved in *Daf1* promoter activity. However, the relative luciferase activity obtained with the p(-179/+85)Luc construct was still elevated, suggesting that regulatory elements involved in basal transcription of the *Daf1* promoter were likely to be contained within this region. This was confirmed with the next deletion to position -18 (p(-18/+85)Luc), as the relative luciferase activities observed with this construct and the control pGL3 vector were almost indistinguishable (Fig. 4B) in all cell lines tested.

Alignment of the -179- to +85-bp murine sequence with that of the rat, human, and chimpanzee was done using the BioEdit Sequence Alignment Editor Software (version 6.0.5) (Fig. 4C). This sequence contains one Ikaros 1 site (-137 to -128), one CREB site (-98 to -91), and four Sp1-binding sites at positions

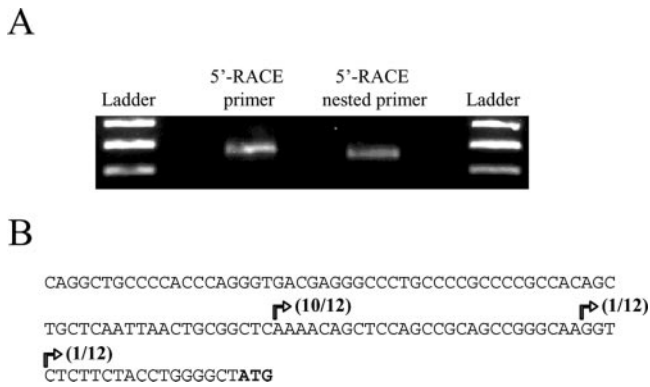


FIGURE 2. Identification of *Daf1* transcription start site. Transcription start was performed using RACE. Total RNA was extracted from mouse spleen tissue and reverse transcription was performed using random primers (N_6). RACE-ready cDNA was then amplified using a forward GeneRacer 5' primer and a reverse *Daf1*-specific primer. Nested PCR was also performed using a forward GeneRacer 5' nested primer and a reverse *Daf1*-specific primer. *A*, PCR products were separated on agarose gel, purified, and cloned into pCR4-TOPO vector. Twelve clones were then sequenced and aligned with the sequence retrieved in Fig. 1. *B*, Transcription starts are represented by broken arrows and the number of clones is shown in parentheses.

–153 to –147 (site A), –109 to –103 (site B), –84 to –76 (site C), and +10 to +16 (site D). Interestingly, Sp1-binding sites B and C show a high sequence identity between all four species (100 and 80%, respectively) while Sp1-binding sites A and D display only moderate sequence conservation (50 and 42.8%, respectively).

Basal murine *Daf1* gene expression is regulated through two Sp1-binding sites

The transcription factor Sp1 is often involved in the basal transcription of TATA-less genes and consequently has been shown to be a key element in the transcription of many housekeeping genes (32, 33). To determine whether Sp1 was a key *cis*-acting transcription factor in the regulation of *Daf1* gene transcription, we used *D. melanogaster* Schneider SL2 cells, known to be deficient in endogenous Sp factors (34). SL2 were transfected with pGL3, p(–18/+85)Luc, p(–179/+85)Luc, p(–619/+85)Luc, and the full-length p(–2408/+85)Luc vectors along with the *Renilla* luciferase containing vector pRL-TK. Interestingly, none of the promoter 5'-deletion constructs produced luciferase activity, indicating that Sp transcription factors are required for *Daf1* promoter activity (Fig. 5). The same *Daf1* luciferase reporter vectors were then cotransfected with increasing amounts of pPacSp1, a vector encoding the Sp1 protein. Cotransfection of p(–18/+85)Luc with pPacSp1 failed to produce luciferase activity above the threshold observed in the absence of pPacSp1 (Fig. 5), confirming that the Sp1 site D located at position +10 to +16 is not involved in basal transcription of *Daf1*. In contrast, when p(–179/+85)Luc was cotransfected with 100 ng of pPacSp1, the relative luciferase activity increased by 265% (Fig. 5), showing that Sp1 binding to one or more of the three Sp1 sites located between –179 and –18 bp (Fig. 4C) is required for basal *Daf1* gene transcription. Similar results were obtained with the p(–619/+85)Luc and p(–2408/+85)Luc constructs, displaying increases of 322 and 331%, respectively, when cotransfected with 100 ng of pPacSp1 (Fig. 5).

To further investigate the contribution of each Sp1-binding site to *Daf1* transcriptional regulation, we performed mutational analysis of the p(–619/+85)Luc construct in which one, two, or all

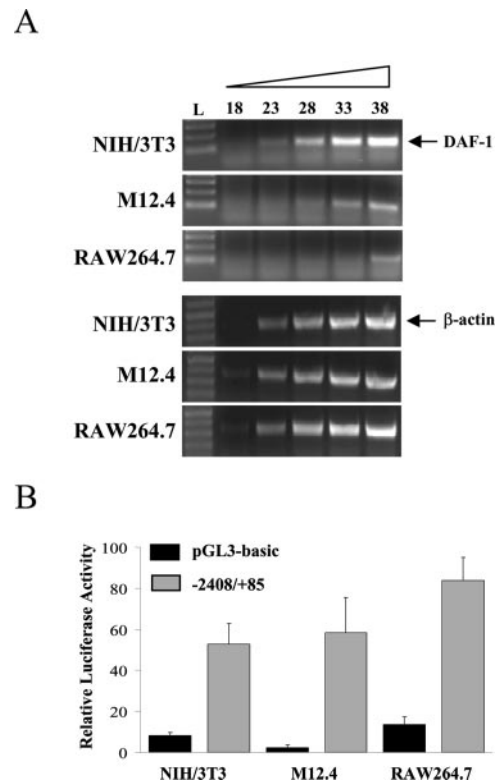


FIGURE 3. *Daf1* expression in murine fibroblasts, B cells, and macrophages. *A*, Constitutive *Daf1* mRNA level. Total RNA was extracted from the indicated cell lines and reverse transcribed. PCR was then performed using both *Daf1*- and β -actin-specific primers for the indicated cycle number. PCR products were run on agarose gel and visualized with ethidium bromide. L represents DNA ladder. *B*, A genomic fragment corresponding to the *Daf1* gene 5' flanking region (–2408/+85 from translational start site) was cloned into the promoterless vector pGL3 encoding firefly luciferase. Either this construct or the pGL3 control vector was transiently transfected into the indicated cell line along with the transfection efficiency control plasmid pRL-TK encoding the *Renilla* luciferase. Luciferase activities were measured 48 h posttransfection. Data (mean \pm SD) have been normalized relative to the *Renilla* luciferase activity.

three Sp1-binding sites were mutated. Mutation of the Sp1-binding sites A or B, or double mutation of both sites A and B (Sp1-A/B mutant) did not produce significant change in luciferase activity compared with the wild-type p(–619/+85)Luc construct in all three cell lines (Fig. 6A). However, mutation within the Sp1-C site significantly reduced the luciferase activity by 46.1% in NIH/3T3, 41.6% in M12.4 and 52.7% in RAW264.7 (all three cell lines, $p < 0.01$) compared with the p(–619/+85)Luc construct suggesting that Sp1 binding to site C contributes significantly to basal transcription of *Daf1*. Similar reduction in the luciferase activities was observed with the Sp1-A/C double mutant. A more dramatic decrease in the promoter activity was detected using the Sp1-B/C double mutant as the luciferase activities obtained with this construct only corresponded to 14.52% in NIH/3T3, 15.27% in M12.4, and 19% in RAW264.7 of the luciferase activity observed with the p(–619/+85)Luc construct. Finally, minimal luciferase activities were obtained in all three cell lines using the triple mutant Sp1-A/B/C, although the difference between this construct and the Sp1-B/C double mutant was only significant in the NIH/3T3 and M12.4 ($p < 0.01$ and $p = 0.023$, respectively) but not in RAW264.7 ($p = 0.093$).

To confirm these findings, we transiently transfected the same deletion mutant constructs into Sp1-deficient Schneider SL2 cells

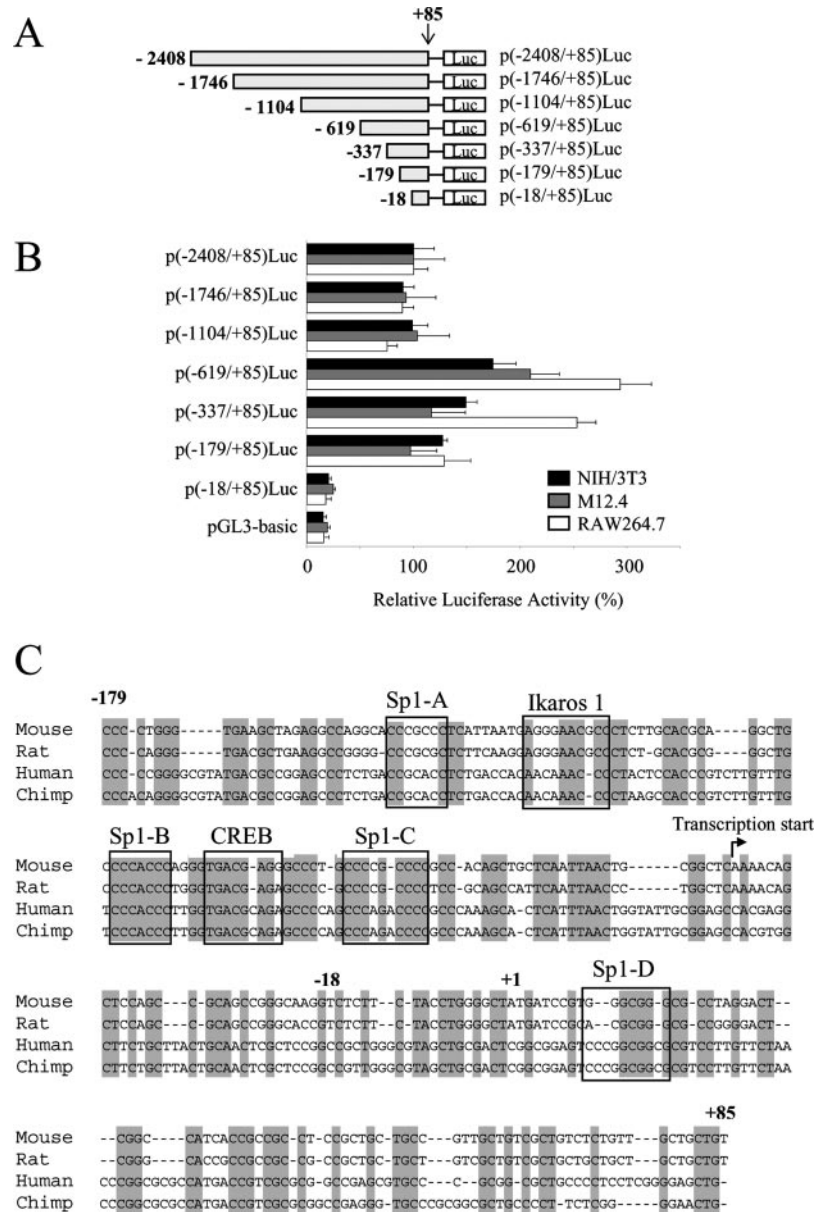


FIGURE 4. Deletion analysis of the Daf1 5'-flanking region. **A**, Schematic representation of Daf1 5' deletion constructs generated by PCR using primers depicted in Fig. 1. **B**, The plasmids containing sequentially deleted fragments of p(-2408/+85)Luc were transiently transfected in the indicated cell lines along with the transfection efficiency control plasmid, pRL-TK encoding the *Renilla* luciferase. Firefly luciferase activities were recorded and normalized using *Renilla* luciferase activities. Data (mean \pm SD) are from quadruplicate transfections representing the percent activity relative to the p(-2408/+85)Luc luciferase activity defined as 100%. **C**, Alignment of the 5'-flanking sequence (-179/+85) of mouse, rat, human, and chimpanzee (chimp.) *DAF* genes. The translation initiation site is indicated by a +1 and the transcription start is designated by a broken arrow. Consensus binding sites for the indicated transcription factors are boxed.

with or without cotransfection with the Sp1-containing vector, pPacSp1. The luciferase activity of the p(-619/+85)Luc vector showed an \sim 3-fold increase when cotransfected with the pPacSp1 plasmid, while luciferase activities of both pGL3 control vector and p(-18/+85)Luc construct remained unchanged (Fig. 6B). As expected, when cotransfected with pPacSp1, the increase obtained with Sp1-A mutant was very similar to that observed with p(-619/+85)Luc vector while it was reduced with both Sp1-C and Sp1-A/C mutants and nearly abolished by either Sp1-B/C or Sp1-A/B/C mutants. However, mutations in Sp1-B and Sp1-A/B significantly decreased the Sp1 effect ($p < 0.01$ and $p = 0.0175$, respectively) compared with the p(-619/+85)Luc vector indicating that mutations in Sp1-binding site B might also affect Daf1 promoter activity. This result differs from that obtained in Fig. 6A because, in all the cell lines tested, Sp1-B by itself did not appear to be involved in the Daf1 promoter activity. Taken together, this result indicates that the basal Daf1 promoter activity is mainly regulated by Sp1-binding sites B and C acting in a synergistic manner.

The transcription factor Sp1 associates with both B and C Sp1-binding sites

To investigate whether Sp1 physically binds to the Sp1-binding sites B (-109 to -103) and C (-84 to -76), we performed a transcription factor ELISA (TF-ELISA) using biotinylated dsDNA containing either the Sp1-binding sites B (Oligo B, Fig. 7A) or C (Oligo C, Fig. 7B). Representative TF-ELISA results depicted in Fig. 7, A and B, showed that Sp1 binding to both Sp1-binding sites B and C increased proportionally with the amount of nuclear extract from all three cell lines. For both oligo B and C, the OD₄₀₅ obtained when using nuclear extract from NIH/3T3 cells was always higher than the OD₄₀₅ recorded with nuclear extracts from M12.4 and RAW264.7 cells suggesting the presence of a higher amount of Sp1 in NIH/3T3 cells (Fig. 7, A and B). This could explain why NIH/3T3 cells constitutively expressed more Daf1 mRNA than M12.4 or RAW264.7 cells (Fig. 3A). Dose response assays were also conducted using increasing amount of rSp1 and, similar to the results obtained with the nuclear extracts, Sp1-DNA

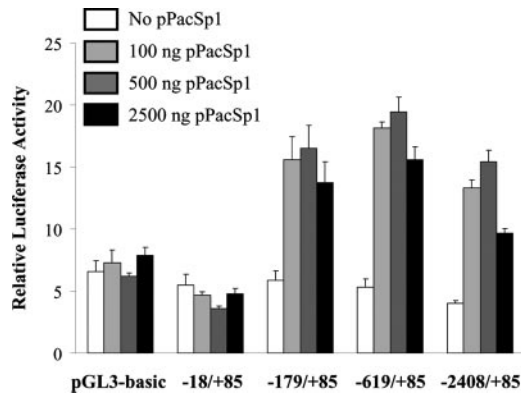


FIGURE 5. Sp1 regulates *Daf1* promoter activity in *Drosophila* Schneider SL2 cells. SL2 cells were transfected with either pGL3, p(-18/+85)Luc, p(-179/+85), p(-619/+85), or p(-2408/+85) constructs and with an increasing amount of the Sp1 containing plasmid pPacSp1 as indicated. Total amount of plasmid DNA transfected was held constant using the corresponding empty vector pPac. *Renilla* luciferase containing vector pRL-TK was also introduced to normalize transfection efficiency. Luciferase activities generated in the presence or absence of pPacSp1 were normalized and data (mean \pm SD) are from quadruplicate transfections.

binding increased proportionally with the amount of rSp1 added (Fig. 7C). Moreover, binding to Sp1 site C was always higher than Sp1 site B for all amounts of rSp1 tested suggesting that Sp1 shows a higher affinity for the Sp1-binding site C (-84 to -76).

To confirm the specificity of Sp1 binding, we performed TF-ELISA using mutated Sp1-binding oligonucleotides and showed that mutation of both the Sp1-binding sites B and C greatly reduced the Sp1-binding affinity compared with the wild-type oligonucleotides (Fig. 7D). We also performed competition experiments in which a gradual decrease in Sp1-binding activity was observed with the addition of increasing amounts of competitor oligonucleotides (Fig. 7E). Taken together, these data demonstrate that the transcription factor Sp1 is capable of binding to the Sp1-binding sites B (-109 to -103) and C (-84 to -76) and support the argument that this transcription factor is directly involved in the regulation of *Daf1* gene expression.

Mutations in the CREB-binding site partially inhibit *Daf1* promoter activity

CREB plays a pivotal role in the transcriptional activity of numerous genes (35) mediated by its binding to the cAMP-response element, a specialized region of genomic DNA that contains the consensus nucleotide sequence TGACGTCA. In the human *DAF* gene, two independent studies have demonstrated that the promoter region containing the cAMP-response element sequence is an important modulator of *Daf* gene transcription (18, 28). A CREB-binding site (-98 to -91) is located within 100 nt of the transcriptional start site of mouse *Daf1* (Fig. 1). This CREB-binding site showed a high degree of sequence conservation between human and rodent species (Fig. 4C). Therefore, to evaluate the importance of the CREB-binding sequence in the murine *Daf1* promoter activity, we prepared p(-619/+85)Luc mutant constructs in which the CREB-binding site was either modified alone or in conjunction with all three Sp1-binding sites. Mutations within the CREB-binding site reduced luciferase activity by 46.7, 44.3, and 40.7%, respectively, in NIH/3T3, M12.4, and RAW264.7 cells relative to the wild-type p(-619/+85)Luc construct (Fig. 8). When the CREB-binding site was mutated together with all three Sp1-binding sites (Sp1-A/B/C), a significant decrease in promoter activity, relative to the Sp1-A/B/C construct ($p < 0.01$ for all three

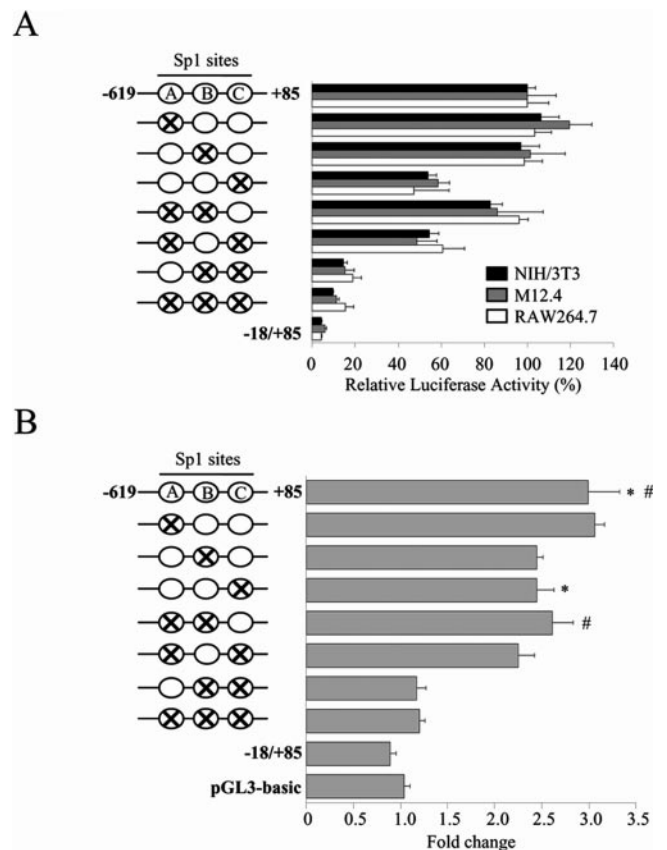


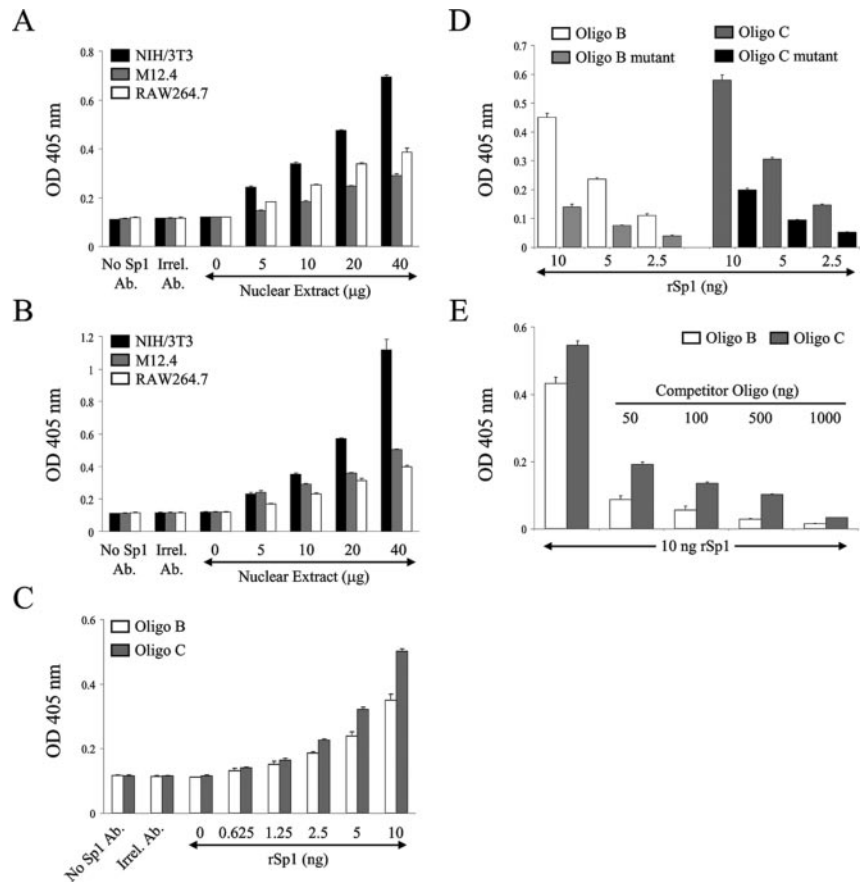
FIGURE 6. *Daf1* promoter activity is regulated through 2 Sp1-binding sites. Sp1 mutational analysis was performed using the p(-619/+85)Luc deletion construct in which either one, two, or all three Sp1 sites were mutated (mutation indicated as X). *A*, The plasmids containing mutated Sp1 sites were transiently transfected into either NIH/3T3, M12.4, or RAW264.7 cells along with the transfection efficiency control vector pRL-TK. Luciferase activities generated were normalized and expressed as the percent activity relative to the p(-619/+85)Luc luciferase activity defined as 100%. Data (mean \pm SD) are from triplicate luciferase assays. *B*, The plasmids containing mutated Sp1 sites were transiently transfected into Schneider SL2 cells along with the control vector pRL-TK. Each Sp1 mutant was also cotransfected with 250 ng of either the Sp1 containing vector pPacSp1 or the empty vector pPac. Luciferase activities were normalized for transfection efficiency and expressed as fold change representing the ratio obtained by dividing the luciferase activity generated in the presence of pPacSp1 by that obtained in the absence of pPacSp1. Data (mean \pm SD) are from triplicate transfections. *A* and *B*, Statistical significance was assigned based on a Student's *t* test with * for $p < 0.01$ and # for $p < 0.05$.

cell lines), was observed suggesting a functional cooperation between Sp1 and CREB transcription factors.

LPS effect on *Daf1* gene expression is abrogated by mutations within Sp1-binding sites

Several previous studies have shown that *Daf1* mRNA can be up-regulated by LPS (36–38), however, little is known about the regulation of *Daf1* gene by LPS in the murine system. NIH/3T3, M12.4, and RAW264.7 cells were cultured with 10 μ g/ml LPS for 24 h and *Daf1* determined by quantitative real-time PCR. As expected, the level of *Daf1* mRNA in untreated (control) NIH/3T3 cells was much higher than in M12.4 and RAW264.7 cells (data not shown) confirming the PCR results shown in Fig. 3A. In NIH/3T3 cells, LPS treatment did not significantly change the level of *Daf1* mRNA while it increased the level by 1.85- and 2.32-fold in M12.4 and RAW264.7 cells, respectively (Fig. 9A). It has been

FIGURE 7. Specific DNA-binding activity of Sp1 to the Sp1-binding sites B (−109/−103) and C (−84/−76) determined by transcription factor ELISA. Biotinylated oligonucleotides containing either Sp1-binding site B (oligo B) or C (oligo C) were generated and immobilized onto a 96-well plate precoated with streptavidin. Nuclear extract was then applied and DNA-Sp1 complexes were detected with an anti-Sp1 Ab followed by a HRP-conjugated secondary Ab. The ABTS substrate solution was then added and color development was measured with a 405 nm microplate reader. Omission of the Sp1-specific Ab and the use of an irrelevant Ab in combination with the highest amount of nuclear extract were used as negative controls. **A**, Dose-response assay using increasing amounts (0–40 μg) of nuclear extract of NIH/3T3, M12.4, and RAW264.7 cells to oligo B. **B**, Dose-response assay using increasing amounts (0–40 μg) of nuclear extract of NIH/3T3, M12.4, and RAW264.7 cells to oligo C. **C**, Dose-response assay using increasing amounts (0–10 ng) of rSp1 to oligo B and C. **D**, Dose-response assay using decreasing amounts (10–2.5 ng) of rSp1 to either wild-type or mutated oligo B and C. **E**, Competition experiment using increasing amounts of non-biotinylated oligonucleotide as competitor to inhibit rSp1 binding to immobilized biotinylated oligo B and C. Data (mean \pm SD) are from triplicate determinations for each ELISA.



shown previously that NIH/3T3 cells lack an intact LPS-signaling pathway (39) which may explain why LPS did not affect *Daf1* gene expression in these cells. We then transiently transfected the p(−2408/+85)Luc vector into the three cell lines and 24 h later cells were treated for an additional 24 h with 10 $\mu\text{g}/\text{ml}$ LPS followed by a dual luciferase assay. The normalized luciferase activity was not affected by LPS treatment in NIH/3T3 cells but was increased in both M12.4 and RAW264.7 cells by 1.97- and 1.85-fold, respectively, matching the data obtained by real-time PCR on the *Daf1* mRNA levels (Fig. 9B). To investigate whether the LPS effect was dependent on the presence of functional Sp1-binding sites, we transfected either the wild-type p(−619/+85)Luc construct or the corresponding Sp1-B/C double and Sp1-A/B/C triple mutants into all three cell lines for 24 h followed by an additional 24 h stimulation with 10 $\mu\text{g}/\text{ml}$ LPS. In accordance with the data presented in Fig. 9, A and B, no LPS effect was detected for all the indicated constructs in the NIH/3T3 cell line. However, in M12.4 and RAW264.7 cells transfected with the p(−619/+85)Luc construct, LPS treatment increased the normalized luciferase activities by 1.82- and 1.95-fold, respectively, and because no LPS effect was observed in p(−18/+85)Luc-transfected cells (Fig. 9C), this would suggest that the region between −619 and −18 bp contains LPS-responsive element(s). Interestingly, inhibition of Sp1 binding by mutating either Sp1-binding sites B and C (Sp1-B/C) or A, B, and C (Sp1-A/B/C) completely abolished the LPS effect observed with the wild-type p(−619/+85)Luc construct suggesting that Sp1 binding to both Sp1-binding sites B (−109 to −103) and C (−84 to −76) is required for LPS-induced *Daf1* transcription.

Discussion

To characterize key regulatory elements involved in the basal transcription of the mouse *Daf1* gene, we cloned and analyzed a 2.5-kb

genomic fragment corresponding to the 5'-flanking region of the *Daf1* gene. Analysis of this fragment revealed that, like its human counterpart, the *Daf1* promoter lacks conventional TATA and

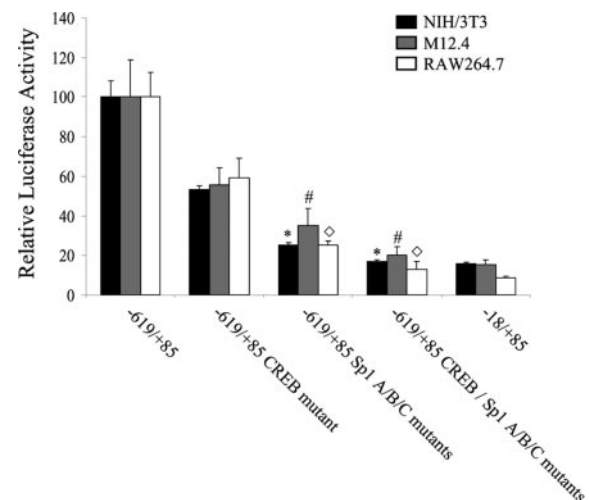


FIGURE 8. CREB-binding site is involved in the basal activity of *Daf1* promoter. The p(−619/+85)Luc construct was used to generate mutant constructs in which the CREB-binding site was either modified alone or in conjunction with all the three Sp1-binding sites. These constructs were then transiently transfected together with the transfection control vector pRL-TK in the indicated cell lines and a dual-luciferase assay performed. Data (mean \pm SD) are from duplicate transfections performed in quadruplicate and expressed as relative luciferase activity representing the percent activity relative to the p(−619/+85)Luc luciferase activity defined as 100%. Statistical significance was assigned based on a Student's *t* test with *, #, and ◇ for $p < 0.01$.

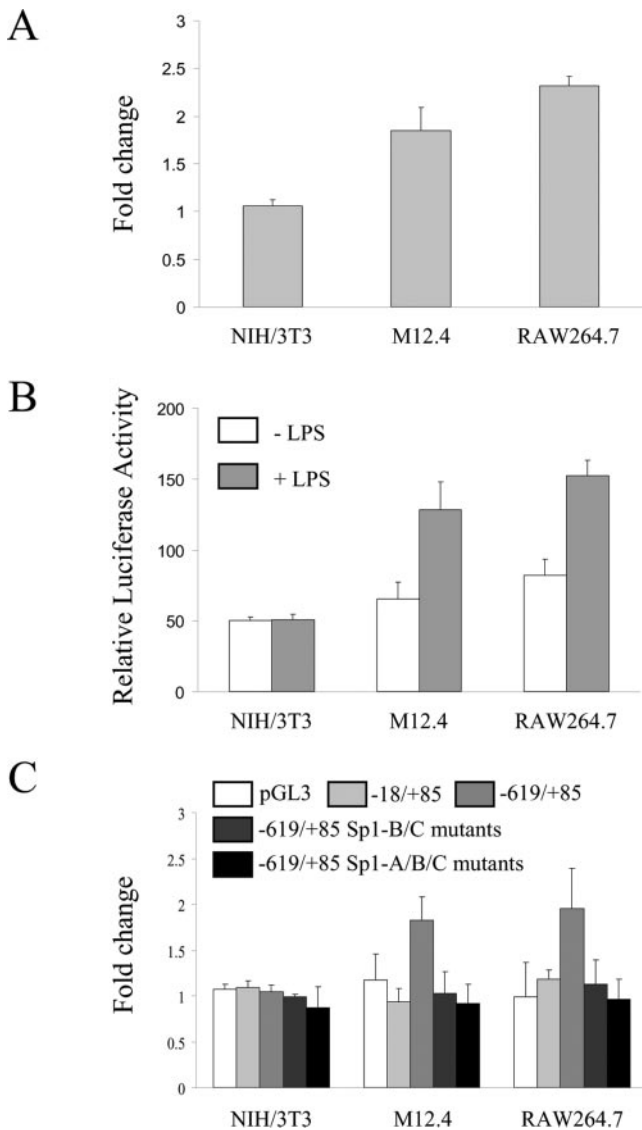


FIGURE 9. LPS effect on *Daf1* gene expression is abolished by mutations in Sp1-binding sites. *A*, Total RNA was extracted from NIH/3T3, M12.4, and RAW264.7 cells stimulated with 10 $\mu\text{g}/\text{ml}$ LPS for 24 h. Quantitative real-time PCR was then performed on reverse-transcribed RNA and *Daf1* mRNA level was normalized using cyclophilin A. Data (mean \pm SD) from triplicate experiments is expressed as fold change over non-LPS treated controls. *B*, The full-length p(-2408/+85)Luc construct was transiently transfected into the indicated cell lines along with the transfection control vector pRL-TK and 24 h later cells were treated or not for an additional 24 h with 10 $\mu\text{g}/\text{ml}$ LPS. Luciferase activities were then measured and normalized for transfection efficiency. Data (mean \pm SD) are from triplicate transfections expressed as relative luciferase activity. *C*, NIH/3T3, M12.4, and RAW264.7 cells were transiently transfected with the indicated constructs and 24 h later, cells were treated or not for an additional 24 h with 10 $\mu\text{g}/\text{ml}$ LPS. Luciferase activities were then measured and normalized for transfection efficiency. Data (mean \pm SD) are from triplicate transfections expressed as fold change corresponding to the ratio of normalized luciferase activities obtained from LPS treated cells to the normalized luciferase activities recorded in nontreated cells.

CCAAT boxes (18). Absence of a consensus TATA box is a feature found in the promoters of other complement regulatory proteins including the membrane cofactor protein (CD46) (40), CD59 (41), CR1/CD35 (42), C1 inhibitor (43), C4b-binding protein (44), factor H (45), and factor I (46). We also found that the mouse *Daf1* promoter contains a GC-rich domain which, in agreement with

previous studies, shows that promoters lacking a TATA box often contain GC-rich regions proximal to their transcription start site (31, 47). Additionally, it has been shown that TATA-less GC-rich promoters are predominantly found in genes that are ubiquitously expressed, particularly those termed housekeeping genes (31). The mouse *Daf1* gene is found to be widely expressed not only in hemopoietic cells but also in a wide variety of other tissues (16, 17). Previous reports have also indicated that the promoters of other members of the complement regulatory protein family, including CD46 (40), CD59 (41), and C1 inhibitor (43), are GC rich as well as being TATA-less.

It has been previously shown that GC-rich promoters that lack a TATA box display multiple transcription start sites (31). RACE analysis, performed on total RNA isolated from DBA/2 splenocytes, identified three different sites of transcription initiation situated 47, 20, and 17 bp upstream of the translational start codon. However, in 10 of 12 clones (~85%), transcription was initiated 47 bp upstream of the ATG codon thus defining the major transcription start site. A previous report described the transcription start of the murine *Daf1* gene as 15 bp upstream of the ATG codon (15). The discrepancy between data presented here and the previous report may be explained by the origin of the total RNA which was, in the first study, isolated from the testes of C57BL/6J mice. In the human *DAF* gene, Ewulonu et al. (28) showed that the main transcription start site was located 82 bp upstream of the ATG initiation codon, while Thomas and Lublin (18) found multiple transcription start sites mapped in a stretch of 10 bp located 87 bp upstream of the translational start codon.

Deletion analysis of the 2.5-kb genomic fragment corresponding to the 5'-flanking region of the *Daf1* gene revealed that gene expression is modulated by both negative and positive regulatory elements located between -1104 to -619 bp and -619 to -18 bp from the ATG codon, respectively. What transcription factor(s) exert a negative regulatory function on the mouse *Daf1* promoter remains to be determined. An inhibitory sequence region, lying between -815 to -355 bp of the translation codon, has also been described in the human *DAF* gene promoter (28). Further deletions showed that the short region located between -179 and -18 bp upstream of the ATG codon was essential for constitutive *Daf1* gene expression because deletion of this region abolished almost all promoter activity. Computational analysis of this core promoter region identified two putative GC boxes (CCCGCCC) located between -153 to -147 and -84 to -76 bp and one GT/CACCC box located between -109 to -103 bp upstream of the translation start codon. These GC-rich promoter elements have been previously described in many genes to be the binding site of the ubiquitously expressed transcription factor Sp1 found to be a key player in the basal transcription of many housekeeping genes (32, 33). To demonstrate that Sp1 was actually involved in the transcription of the mouse *Daf1* gene, we used several approaches. First, we showed that the lack of promoter activity observed in Sp-deficient *Drosophila* SL2 cells transfected with *Daf1* reporter constructs was reversed by the addition of exogenous Sp1. Second, we performed a mutational analysis of the Sp1-binding sites and demonstrated that the promoter activity was markedly reduced when both the GC box located -84 to -76 bp and the GT box located -109 to -103 bp from the ATG codon were mutated simultaneously, with mutation of the most proximal Sp1-binding site having the largest effect. Third, we confirmed by transcription factor ELISA that Sp1 is capable of binding to both Sp1-binding sites.

Previous studies have determined that Sp1-dependent transcriptional activation of TATA-less promoters is mediated by the interaction of the glutamine-rich domain of Sp1 and TATA-binding

protein-associated factors subunits of the RNA polymerase II basal transcription factor TFIID (48, 49). Moreover, Ryu et al. (50) showed that the cofactor complex CRSP (cofactor required for Sp1 activation) was also required for efficient transcriptional activation by Sp1. Additionally, it has been demonstrated that the binding of Sp1 to multiple binding sites is often essential for significant transcription activity (51–53). This cooperative effect between Sp1-binding sites to achieve full gene expression has been shown to be mediated via the formation of Sp1-Sp1 complexes (54). However, in some cases, the most proximal Sp1-binding site seems to be more important, if not absolutely required, for transcription activity (31, 55, 56). We demonstrated in this study that the GC box located –37 to –29 bp upstream of the transcriptional start site was the major Sp1-binding site for transcription activity because mutation of this site reduced promoter activity by ~50% in all the cell lines tested while mutations in the two other Sp1-binding sites did not significantly influence gene transcription. Consistent with this idea, we also demonstrated that the binding affinity of Sp1 for the most proximal Sp1-binding site was higher than for the one located –62 to –56 bp from the transcriptional start site. Furthermore, we showed that the increased promoter activity observed in LPS-treated cells was totally abolished when both Sp1 sites were mutated, indicating that functional Sp1 sites are required for the *Daf1* promoter to function properly. Similarly, Tone et al. (57) showed that the LPS effect on *CD40* gene expression was greatly reduced by introducing mutations into Sp1-binding sites.

In the human *DAF* gene, Thomas and Lublin (18) have identified three separate regions controlling DAF promoter activity. The first region, located between –54 and –34 bp from the transcription start, was shown to be necessary for low level transcription and to contain an Sp1-binding site. A second region, between –77 and –54 bp, encompassing both CREB- and AP-1-binding sites, was capable of up-regulating transcriptional activity. The same CREB-binding site was shown to be likely involved in cAMP-mediated up-regulation of the promoter activity (28). In a comparative sequence analysis, we noted that the region containing the CREB-binding site, as well as both Sp1-binding sites, exhibits high sequence homology between human and mouse DAF. To assess the role of the CREB-binding site in the murine promoter, we generated constructs in which the CREB-binding site was mutated and showed that this mutant construct displayed a 40% decrease in promoter activity indicating that, as in human, the CREB-binding site is involved in the up-regulation of basal transcriptional activity of murine *Daf1* gene. This supports previous studies which have revealed that functional cooperation between Sp1 and CREB is critical in driving gene expression (58, 59). Interestingly, the constitutive activation domain of CREB has been shown to interact with the TATA-binding protein-associated factor subunit and to mediate the recruitment of the RNA polymerase II complex (60). Finally, a third region located between –206 and –77 bp and containing potential enhancer element(s) was also identified in the human *DAF* gene. Interestingly, this region contains a GT/CACCC box consensus sequence perfectly conserved with that described in this study, and shown to be significantly involved in the transcription of the murine *Daf1* gene.

In summary, our data clearly show that the transcriptional activity of the mouse *Daf1* promoter requires the functional cooperation of two Sp1-binding sites, a feature frequently observed in mammalian GC-rich, TATA-less promoters. Sp1 also contributes to the induction of *Daf1* transcription by LPS. Furthermore, CREB appears to be an important modulator of transcriptional activity by enhancing the basal transcription activity supported by Sp1. These findings not only identify the mechanism that drives basal expression but also provide the framework to explain the molecular basis

for the regulation of *Daf1* gene expression. These initial observations should facilitate future studies aimed at examining the regulation of *Daf1* expression in immune responses.

Acknowledgments

We gratefully appreciate the technical assistance of E. K. Jung and C. Toomey. We thank Prof. R. H. Scheuermann (University of Texas Southwestern Medical Center, TX) for B cell line M12.4 and Prof. Guntram Suske (Philipps University, Marburg, Germany) for providing pPac and pPacSp1. Finally, we thank Prof. J. N. Buxbaum, Dr. J. S. Friedman, and Dr. K. V. Morris for critical reading and helpful comments on the manuscript. This is publication 18184-MEM from the Department of Molecular and Experimental Medicine (W. M. Keck Autoimmune Disease Center, The Scripps Research Institute).

Disclosures

The authors have no financial conflict of interest.

References

- Lublin, D. M., and J. P. Atkinson. 1989. Decay-accelerating factor: biochemistry, molecular biology, and function. *Annu. Rev. Immunol.* 7: 35–58.
- Song, W. C. 2004. Membrane complement regulatory proteins in autoimmune and inflammatory tissue injury. *Curr. Dir. Autoimmun.* 7: 181–199.
- Liu, J., T. Miwa, B. Hilliard, Y. Chen, J. D. Lambris, A. D. Wells, and W. C. Song. 2005. The complement inhibitory protein DAF (CD55) suppresses T cell immunity in vivo. *J. Exp. Med.* 201: 567–577.
- Heeger, P. S., P. N. Lalli, F. Lin, A. Valujskikh, J. Liu, N. Muqim, Y. Xu, and M. E. Medof. 2005. Decay-accelerating factor modulates induction of T cell immunity. *J. Exp. Med.* 201: 1523–1530.
- Lea, S. 2002. Interactions of CD55 with non-complement ligands. *Biochem. Soc. Trans.* 30: 1014–1019.
- Hamann, J., B. Vogel, G. M. van Schijndel, and R. A. van Lier. 1996. The seven-span transmembrane receptor CD97 has a cellular ligand (CD55, DAF). *J. Exp. Med.* 184: 1185–1189.
- Visser, L., A. F. de Vos, J. Hamann, M. J. Mielief, M. van Meurs, R. A. van Lier, J. D. Laman, and R. Q. Hintzen. 2002. Expression of the EGF-TM7 receptor CD97 and its ligand CD55 (DAF) in multiple sclerosis. *J. Neuroimmunol.* 132: 156–163.
- Leemans, J. C., A. A. te Velde, S. Florquin, R. J. Bennink, K. de Bruin, R. A. van Lier, T. van der Poll, and J. Hamann. 2004. The epidermal growth factor-seven transmembrane (EGF-TM7) receptor CD97 is required for neutrophil migration and host defense. *J. Immunol.* 172: 1125–1131.
- Davis, L. S., S. S. Patel, J. P. Atkinson, and P. E. Lipsky. 1988. Decay-accelerating factor functions as a signal transducing molecule for human T cells. *J. Immunol.* 141: 2246–2252.
- Shibuya, K., T. Abe, and T. Fujita. 1992. Decay-accelerating factor functions as a signal transducing molecule for human monocytes. *J. Immunol.* 149: 1758–1762.
- Shenoy-Scaria, A. M., J. Kwong, T. Fujita, M. W. Olszowy, A. S. Shaw, and D. M. Lublin. 1992. Signal transduction through decay-accelerating factor: interaction of glycosyl-phosphatidylinositol anchor and protein tyrosine kinases p56^{lck} and p59^{lyn}. *J. Immunol.* 149: 3535–3541.
- Post, T. W., M. A. Arce, M. K. Liszewski, E. S. Thompson, J. P. Atkinson, and D. M. Lublin. 1990. Structure of the gene for human complement protein decay accelerating factor. *J. Immunol.* 144: 740–744.
- Nicholson-Weller, A., J. P. March, C. E. Rosen, D. B. Spicer, and K. F. Austen. 1985. Surface membrane expression by human blood leukocytes and platelets of decay-accelerating factor, a regulatory protein of the complement system. *Blood* 65: 1237–1244.
- Medof, M. E., E. I. Walter, J. L. Rutgers, D. M. Knowles, and V. Nussenzweig. 1987. Identification of the complement decay-accelerating factor (DAF) on epithelium and glandular cells and in body fluids. *J. Exp. Med.* 165: 848–864.
- Spicer, A. P., M. F. Seldin, and S. J. Gendler. 1995. Molecular cloning and chromosomal localization of the mouse decay-accelerating factor genes: duplicated genes encode glycosylphosphatidylinositol-anchored and transmembrane forms. *J. Immunol.* 155: 3079–3091.
- Lin, F., Y. Fukuoka, A. Spicer, R. Ohta, N. Okada, C. L. Harris, S. N. Emancipator, and M. E. Medof. 2001. Tissue distribution of products of the mouse decay-accelerating factor (DAF) genes: exploitation of a *Daf1* knock-out mouse and site-specific monoclonal antibodies. *Immunology* 104: 215–225.
- Miwa, T., X. Sun, R. Ohta, N. Okada, C. L. Harris, B. P. Morgan, and W. C. Song. 2001. Characterization of glycosylphosphatidylinositol-anchored decay accelerating factor (GPI-DAF) and transmembrane DAF gene expression in wild-type and GPI-DAF gene knockout mice using polyclonal and monoclonal antibodies with dual or single specificity. *Immunology* 104: 207–214.
- Thomas, D. J., and D. M. Lublin. 1993. Identification of 5'-flanking regions affecting the expression of the human decay accelerating factor gene and their role in tissue-specific expression. *J. Immunol.* 150: 151–160.
- Song, W. C., C. Deng, K. Raszmann, R. Moore, R. Newbold, J. A. McLachlan, and M. Negishi. 1996. Mouse decay-accelerating factor: selective and tissue-specific induction by estrogen of the gene encoding the glycosylphosphatidylinositol-anchored form. *J. Immunol.* 157: 4166–4172.

20. Spiller, O. B., O. Criado-Garcia, S. Rodriguez De Cordoba, and B. P. Morgan. 2000. Cytokine-mediated up-regulation of CD55 and CD59 protects human hepatoma cells from complement attack. *Clin. Exp. Immunol.* 121: 234–241.
21. Cocuzzi, E. T., D. S. Bardenstein, A. Stavitsky, N. Sundarraj, and M. E. Medof. 2001. Upregulation of DAF (CD55) on orbital fibroblasts by cytokines: differential effects of TNF- β and TNF- α . *Curr. Eye Res.* 23: 86–92.
22. Ahmad, S. R., E. A. Lidington, R. Ohta, N. Okada, M. G. Robson, K. A. Davies, M. Leitges, C. L. Harris, D. O. Haskard, and J. C. Mason. 2003. Decay-accelerating factor induction by tumour necrosis factor- α , through a phosphatidylinositol-3 kinase and protein kinase C-dependent pathway, protects murine vascular endothelial cells against complement deposition. *Immunology* 110: 258–268.
23. Holla, V. R., D. Wang, J. R. Brown, J. R. Mann, S. Katkuri, and R. N. DuBois. 2005. Prostaglandin E₂ regulates the complement inhibitor CD55/decay-accelerating factor in colorectal cancer. *J. Biol. Chem.* 280: 476–483.
24. Andoh, A., K. Kinoshita, I. Rosenberg, and D. K. Podolsky. 2001. Intestinal trefoil factor induces decay-accelerating factor expression and enhances the protective activities against complement activation in intestinal epithelial cells. *J. Immunol.* 167: 3887–3893.
25. Saklatvala, J., J. Dean, and A. Clark. 2003. Control of the expression of inflammatory response genes. *Biochem. Soc. Symp.* 70: 95–106.
26. Kendall, G., H. Crankson, E. Ensor, D. M. Lublin, and D. S. Latchman. 1996. Activation of the gene encoding decay accelerating factor following nerve growth factor treatment of sensory neurons is mediated by promoter sequences within 206 bases of the transcriptional start site. *J. Neurosci. Res.* 45: 96–103.
27. Louis, N. A., K. E. Hamilton, T. Kong, and S. P. Colgan. 2005. HIF-dependent induction of apical CD55 coordinates epithelial clearance of neutrophils. *FASEB J.* 19: 950–959.
28. Ewulonu, U. K., L. Ravi, and M. E. Medof. 1991. Characterization of the decay-accelerating factor gene promoter region. *Proc. Natl. Acad. Sci. USA* 88: 4675–4679.
29. Birney, E., D. Andrews, M. Caccamo, Y. Chen, L. Clarke, G. Coates, T. Cox, F. Cunningham, V. Curwen, T. Cutts, et al. 2006. Ensembl 2006. *Nucleic Acids Res.* 34: D556–D561.
30. Hibma, M. H., S. J. Ely, and L. Crawford. 1994. A non-radioactive assay for the detection and quantitation of a DNA binding protein. *Nucleic Acids Res.* 22: 3806–3807.
31. Blake, M. C., R. C. Jambou, A. G. Swick, J. W. Kahn, and J. C. Azizkhan. 1990. Transcriptional initiation is controlled by upstream GC-box interactions in a TATAA-less promoter. *Mol. Cell. Biol.* 10: 6632–6641.
32. Suske, G. 1999. The Sp-family of transcription factors. *Gene* 238: 291–300.
33. Philipsen, S., and G. Suske. 1999. A tale of three fingers: the family of mammalian Sp/KKLF transcription factors. *Nucleic Acids Res.* 27: 2991–3000.
34. Suske, G. 2000. Transient transfection of Schneider cells in the study of transcription factors. *Methods Mol. Biol.* 130: 175–187.
35. Johannessen, M., M. P. Delhandi, and U. Moens. 2004. What turns CREB on? *Cell. Signal.* 16: 1211–1227.
36. Moutabarrik, A., I. Nakanishi, M. Namiki, T. Hara, M. Matsumoto, M. Ishibashi, A. Okuyama, D. Zaid, and T. Seya. 1993. Cytokine-mediated regulation of the surface expression of complement regulatory proteins, CD46(MCP), CD55(DAF), and CD59 on human vascular endothelial cells. *Lymphokine Cytokine Res.* 12: 167–172.
37. Iborra, A., M. Mayorga, N. Llobet, and P. Martinez. 2003. Expression of complement regulatory proteins [membrane cofactor protein (CD46), decay accelerating factor (CD55), and protectin (CD59)] in endometrial stressed cells. *Cell. Immunol.* 223: 46–51.
38. Li, W., T. Tada, T. Miwa, N. Okada, J. Ito, H. Okada, H. Tateyama, and T. Eimoto. 1999. mRNA expression of complement components and regulators in rat arterial smooth muscle cells. *Microbiol. Immunol.* 43: 585–593.
39. Krays, V., P. Thompson, and B. Beutler. 1993. Extinction of the tumor necrosis factor locus, and of genes encoding the lipopolysaccharide signaling pathway. *J. Exp. Med.* 177: 1383–1390.
40. Cui, W., D. Hourcade, T. Post, A. C. Greenlund, J. P. Atkinson, and V. Kumar. 1993. Characterization of the promoter region of the membrane cofactor protein (CD46) gene of the human complement system and comparison to a membrane cofactor protein-like genetic element. *J. Immunol.* 151: 4137–4146.
41. Holguin, M. H., C. B. Martin, T. Eggett, and C. J. Parker. 1996. Analysis of the gene that encodes the complement regulatory protein, membrane inhibitor of reactive lysis (CD59): identification of an alternatively spliced exon and characterization of the transcriptional regulatory regions of the promoter. *J. Immunol.* 157: 1659–1668.
42. Kim, J. H., S. Lee, and S. Y. Choe. 1999. Characterization of the human *CR1* gene promoter. *Biochem. Mol. Biol. Int.* 47: 655–663.
43. Zahedi, K., A. E. Prada, and A. E. Davis, 3rd. 1994. Transcriptional regulation of the C1 inhibitor gene by γ -interferon. *J. Biol. Chem.* 269: 9669–9674.
44. Arenzana, N., and S. Rodriguez de Cordoba. 1996. Promoter region of the human gene coding for β -chain of C4b binding protein: hepatocyte nuclear factor-3 and nuclear factor- κ B/CTF transcription factors are required for efficient expression of C4BPB in HepG2 cells. *J. Immunol.* 156: 168–175.
45. Williams, S. A., and D. P. Vik. 1997. Characterization of the 5' flanking region of the human complement factor H gene. *Scand. J. Immunol.* 45: 7–15.
46. Minta, J. O., M. Fung, S. Turner, R. Eren, L. Zemach, M. Rits, and G. Goldberger. 1998. Cloning and characterization of the promoter for the human complement factor I (C3b/C4b inactivator) gene. *Gene* 208: 17–24.
47. Smale, S. T., and J. T. Kadonaga. 2003. The RNA polymerase II core promoter. *Annu. Rev. Biochem.* 72: 449–479.
48. Pugh, B. F., and R. Tjian. 1991. Transcription from a TATA-less promoter requires a multisubunit TFIID complex. *Genes Dev.* 5: 1935–1945.
49. Emami, K. H., T. W. Burke, and S. T. Smale. 1998. Sp1 activation of a TATA-less promoter requires a species-specific interaction involving transcription factor IID. *Nucleic Acids Res.* 26: 839–846.
50. Ryu, S., S. Zhou, A. G. Ladurner, and R. Tjian. 1999. The transcriptional cofactor complex CRSP is required for activity of the enhancer-binding protein Sp1. *Nature* 397: 446–450.
51. Carcedo, M. T., J. M. Iglesias, P. Bances, R. O. Morgan, and M. P. Fernandez. 2001. Functional analysis of the human annexin A5 gene promoter: a downstream DNA element and an upstream long terminal repeat regulate transcription. *Biochem. J.* 356: 571–579.
52. Koga, T., M. A. Suico, H. Nakamura, M. Taura, Z. Lu, T. Shuto, T. Okiyoned, and H. Kai. 2005. Sp1-dependent regulation of myeloid Elf-1 like factor in human epithelial cells. *FEBS Lett.* 579: 2811–2816.
53. Boisclair, Y. R., A. L. Brown, S. Casola, and M. M. Rechler. 1993. Three clustered Sp1 sites are required for efficient transcription of the TATA-less promoter of the gene for insulin-like growth factor-binding protein-2 from the rat. *J. Biol. Chem.* 268: 24892–24901.
54. Courey, A. J., D. A. Holtzman, S. P. Jackson, and R. Tjian. 1989. Synergistic activation by the glutamine-rich domains of human transcription factor Sp1. *Cell* 59: 827–836.
55. Chen, X., J. C. Azizkhan, and D. C. Lee. 1992. The binding of transcription factor Sp1 to multiple sites is required for maximal expression from the rat transforming growth factor α promoter. *Oncogene* 7: 1805–1815.
56. Dusing, M. R., and D. A. Wiginton. 1994. Sp1 is essential for both enhancer-mediated and basal activation of the TATA-less human adenosine deaminase promoter. *Nucleic Acids Res.* 22: 669–677.
57. Tone, M., Y. Tone, J. M. Babik, C. Y. Lin, and H. Waldmann. 2002. The role of Sp1 and NF- κ B in regulating CD40 gene expression. *J. Biol. Chem.* 277: 8890–8897.
58. Nagata, D., E. Suzuki, H. Nishimatsu, H. Satonaka, A. Goto, M. Omata, and Y. Hirata. 2001. Transcriptional activation of the cyclin D1 gene is mediated by multiple cis-elements, including Sp1 sites and a cAMP-responsive element in vascular endothelial cells. *J. Biol. Chem.* 276: 662–669.
59. Lui, W. Y., K. L. Sze, and W. M. Lee. 2006. Nectin-2 expression in testicular cells is controlled via the functional cooperation between transcription factors of the Sp1, CREB, and AP-1 families. *J. Cell. Physiol.* 207: 144–157.
60. Felinski, E. A., J. Kim, J. Lu, and P. G. Quinn. 2001. Recruitment of an RNA polymerase II complex is mediated by the constitutive activation domain in CREB, independently of CREB phosphorylation. *Mol. Cell. Biol.* 21: 1001–1010.